



RESPONSE AND DAMAGE OF BASE-ISOLATED BUILDINGS SUBJECTED TO EXTREMELY LARGE EARTHQUAKES

Peng PAN¹, Nariaki NAKAYASU², and Masayoshi NAKASHIMA³

SUMMARY

The paper examines two issues of concern regarding the application of base-isolated building structures, i.e. collision of the base-isolated structure with the surrounding walls when subjected to near-fault ground motions, and effects of vertical ground motions on the responses of superstructures. Behavior involving collision is affected greatly by the horizontal force resisting characteristics of the walls including the soils behind, and the number of collisions is limited to one or two in most cases. Vertical ground motions do not affect the maximum story drifts of the superstructure. Horizontal ground motions cause tensile forces in the base-isolators for tall superstructures because of overturning effects, whereas vertical ground motions only do not produce tensile forces in the base-isolators. Floor vertical vibrations in the superstructure are not affected by tensions that would occur in base-isolators.

INTRODUCTION

In Japan, seismic-isolation has been accepted as an appealing design alternative for enhancing both the seismic safety and functionality of building structures against larger earthquake motions. Over 150 new base-isolation projects are implemented every year, and more than 1,000 base-isolated buildings have been constructed after the 1995 Kobe earthquake [1]. Two issues of concern, however, are addressed constantly with respect to such recent applications. One is the effect of near-fault motions including large pulses [2], and the other is the effect of vertical ground motions. The former involves possible collisions against the surrounding retaining walls, and this is directly associated with damage and human safety. The latter is essentially a weak point of base-isolation techniques, involving concerns about the functionality of base-isolated structures [3]. This paper presents numerical investigations into the two issues and examines how seriously we shall consider these effects. In the first part, a base-isolated structure having a five-story RC superstructure was analyzed for its responses when collided with the

¹ Graduate Student, Department of Architecture and Architectural Systems, Kyoto Univ., Kyoto, Japan
Email: pan@steel.mbox.media.kyoto-u.ac.jp

² Graduate Student, Department of Architecture and Architectural Systems, Kyoto Univ., Kyoto, Japan
Email: nspock@alpha.ocn.ne.jp

³ Professor, Disaster Prevention Research Institute, Kyoto Univ., Kyoto, Japan.
Email: nakashima@archi.kyoto-u.ac.jp

surrounding retaining walls. Recorded near-fault ground motions (the fault-normal components) were adopted for the analysis, and the resisting characteristics of the walls including the soils behind were evaluated from the associated FEM analysis. In the second part, two base-isolated structures featured with superstructures of a four-stories and a twelve-stories steel moment frames were analyzed for their responses when subjected to horizontal and vertical ground motions simultaneously. Hysteretic behavior of base-isolators subjected to both the axial and horizontal loads was modeled carefully and incorporated into dynamic response analyses.

EFFECTS OF COLLISION

Analyzed Structure

Near-fault ground motions are characterized by short duration and large velocity of primary motions. Figure 1 shows the 5% damping displacement spectra of twenty nine near-fault ground motions recorded in 1994 Northridge, 1995 Kobe, and 1999 Chi-Chi earthquakes [4]. It is notable that many of the ground motions have large displacements in periods between two to five seconds. When the horizontal deformations of the base-isolation layer exceed the clearance between the structure's edge and the surrounding retaining walls, the structure shall collide the walls.

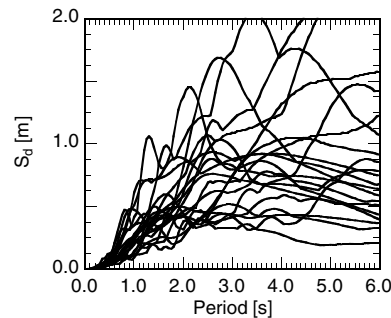


Fig. 1. 5% displacement spectra of near-fault ground motions

According to the preliminary analyses and tests conducted separately [5], damage to the superstructure after collision is affected a great deal by the resistance characteristics of the walls including the soils behind the walls. To quantify this, finite element analyses [6] were carried out for soils. Figure 2(a) shows an example discretization of the soils, and relationships between the force (applied to the top of the soil) and corresponding horizontal displacement were obtained. Relationships between the force and horizontal displacement of RC retaining walls were also obtained, with the walls taken as cantilever beams. Figure 2(b) shows example relationships of the soils and RC walls. It is notable that soils are significantly stronger than the walls. The overall force-displacement relationship of the RC wall and soils is taken to be the parallel sum of the two relationships. A parametric study was conducted for characterization of the relationship, with the type of soil and height of walls as major variables, and the following observations were obtained. The relationship can be reasonably approximated to be linear-elastic and perfect-plastic. The elastic stiffness is about 30 to 60% of the stiffness of the superstructure whose first natural period is 0.5 sec. The strength is about 60 to 300% of the same superstructure having a strength that corresponds to 0.3 in the base shear coefficient. A medium-rise base-isolated structure was adopted as an example to examine the response behavior when subjected to near-fault ground motions. The superstructure analyzed was a five-story RC frame having a yield base shear of 0.3 and the natural period of 0.5 sec. The structure was treated as a planar structure. The base-isolation layer was modeled to be bilinear, with the yield strength equal to 0.05 times the total weight. The natural period of the base-isolated structure (when the superstructure was taken to be rigid) was 4.0 sec with respect to the second stiffness of the base-isolation layer. These properties are typical of base-isolated structures designed in Japan [1].

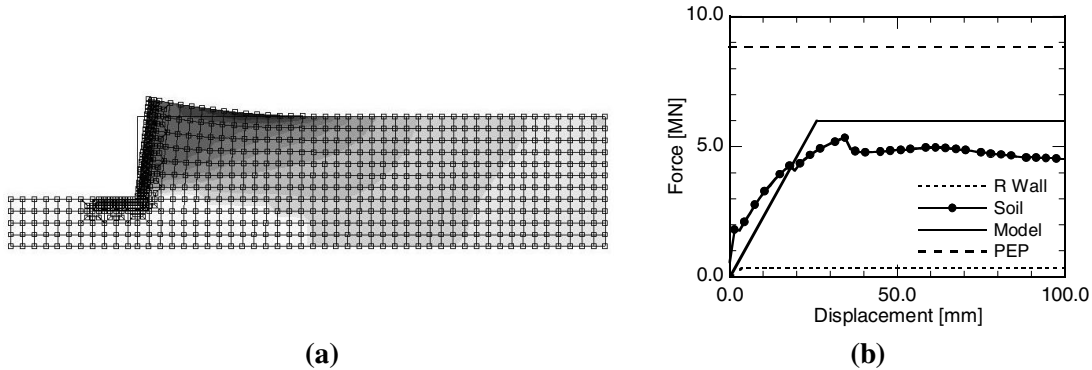


Fig. 2. Horizontal force resistance characteristics of RC wall and soils: (a) soil discretization; (b) horizontal resistance.

Responses Involving Collision

The base-isolated structure was analyzed for the twenty-nine near-fault ground motions (Fig. 1). It was found that fifteen out of twenty-nine motions caused maximum horizontal deformations of the base-isolation layer not smaller than 0.5 m, which is a typical distance of clearance between the structure and surrounding walls. The same structure was analyzed again with the effects of the surrounding walls also taken into account. The retaining wall (including the soils behind) on each size of the structure was modeled as a bilinear spring as shown in Fig. 2(b), and the spring was set to be located with a distance of 0.5 m from the structure when it was at rest. The spring was arranged on each side of the structure. As long as the horizontal deformation of the base-isolation layer was not greater than 0.5 m in the absolute value, the spring did not take any resistance, but once the deformations exceeded 0.5 m, resistance was provided to the responding structure from the walls. Figure 3 shows example responses: Fig. 3(a) shows the displacement time history of the base-isolation layer, and Fig. 3(b) the maximum story drift distribution of the superstructure along the height. For comparison, responses when not collided with the surrounding walls are also presented. The figures indicate that the number of collisions is only two, the base-isolation layer responds very similar regardless of collisions; the maximum story drifts of the superstructure increase with collisions, and the increase is more notable for lower stories.

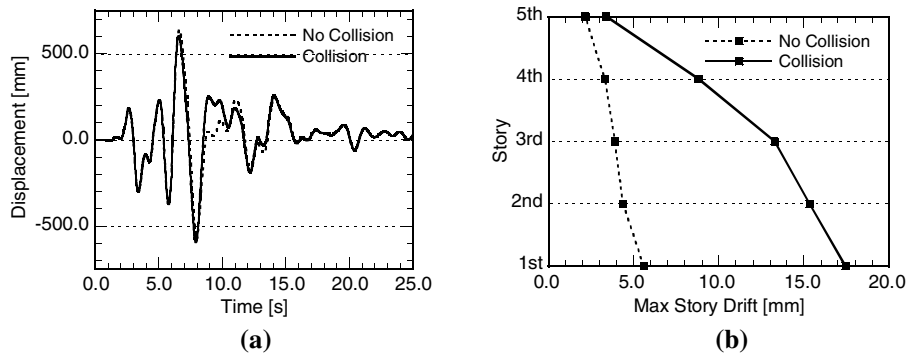


Fig. 3. Responses with collision: (a) displacement time histories; (b) maximum story drifts in superstructure

For the same base-isolated structure, the stiffness and strength of the surrounding walls were taken as variables, and changes in response of the structure were examined as shown in Fig. 4. Figures 4(a) and (b) are the responses of the base-isolation layer and the first story of the superstructure, respectively. The

ordinate and abscissa are the relative strength and stiffness of the walls. Stiff and strong walls (toward the upper right in the figures)) give smaller maximum horizontal displacements to the base-isolation layer but larger story drifts to the superstructure (particularly to the first story). Trade-off in damage between the base-isolation layer and superstructure is notable.

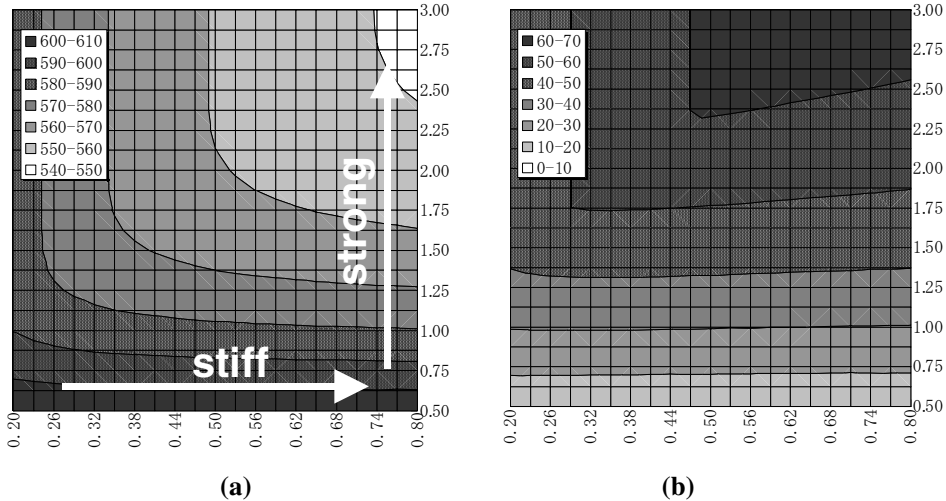


Fig. 4. Effect of wall/soil stiffness and strength on response:
(a) base-isolation layer's maximum horizontal displacement; (b) first story's maximum story drift
(Numbers appearing in inset indicate the displacement in mm.).

To further examine the behavior involving collisions, the responses of the base-isolated structure were analyzed, with the level of ground motions increased successively. Six ground motions recorded in the 1995 Kobe earthquake and causing the maximum horizontal deformations not smaller than 0.5 m in the base-isolation layer were adopted in the analysis. First, the magnitude of each ground motion was adjusted so that the base-isolation layer would reach the maximum horizontal deformation of 0.5 m, then the magnitude was increased successively up to that corresponding to the maximum horizontal deformation of 0.75 m if collision did not occur. Figure 5 shows thus obtained responses, with the magnitude of the ground motion in the abscissa (as the maximum horizontal displacement of the base-isolation layer without collisions) and the maximum responses in the ordinate: the horizontal deformation of the base-isolation layer when collided for Fig. 5(a) and the maximum story drift angle for Fig. 5(b). Except for one ground motion (designated as Fn-ekb), all responses are very similar.

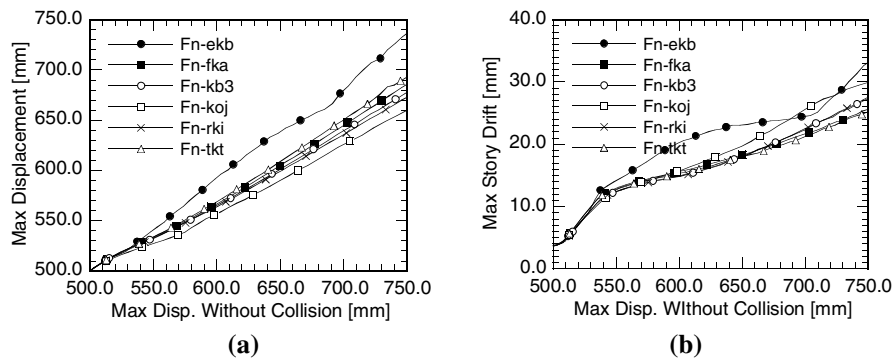


Fig. 5. Responses involving collisions with respect to input level:
base-isolation layer's maximum horizontal displacement; (b) first story's maximum story drift

Figure 6 shows the number of collisions in the responses. Except for Fn-ekb, the number is limited to just one or two even for the magnitude of ground motions that will lead the base-isolation layer to 0.75 m in the horizontal deformation. This seems to be the key to interpret the relatively same responses obtained for most cases with collisions (Fig. 5). Figure 6(b) is the number of collisions obtained for Fn-ekb, showing many rounds of collisions. This resulted in a larger response relative to the other ground motions (Fig. 5). Recognizing the fact that the number of collisions is limited (to one to two), the writers proposed a relatively simple procedure to estimate the maximum responses (for both the base-isolation layer and superstructure) without the exact analysis involving collisions. The details of the procedure is found elsewhere [7].

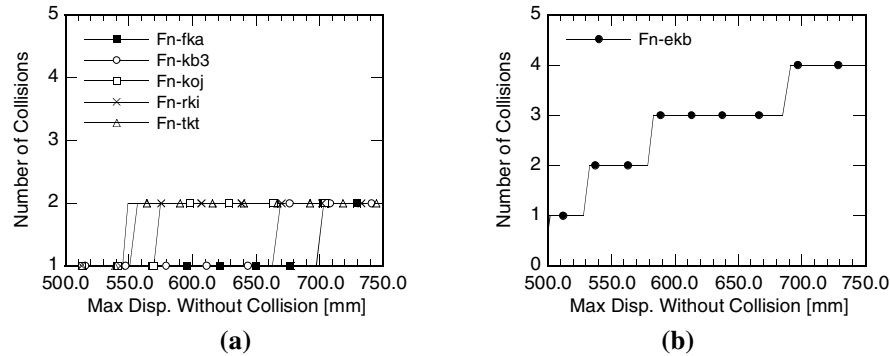


Fig. 6. Number of collisions:
(a) with one or two collisions; (b) with multiple collisions

EFFECTS OF VERTICAL GROUND MOTIONS

Analyzed structure

To explore the effects of vertical motion on the response of base-isolated structures, two base-isolated steel moment frames shown in Fig. 7 (a) and (b) were adopted as representative structures. They were designated as BI-04, and BI-12, respectively. BI-04 was a four-stories, four-spans frame, and BI-12 was twelve-stories, four-spans frame. Both frames were isolated by lead rubber bearings (LRBs), and treated as planar frames. The natural periods of the superstructures in the base-fixed condition are shown in Table 1. The first vertical vibration period is 0.24 sec for BI-04 and 0.25 sec for BI-12. The corresponding vibration modes are primarily the beam vertical vibration for BI-04, and the combined beam and column vertical vibration for BI-12. The natural periods of the base-isolated structures are also shown in Table 1. The horizontal periods are given for rubber's horizontal shear strains of 10%, 100%, and 250%, and the vertical periods are for the compressive vertical stiffness of the base-isolators.

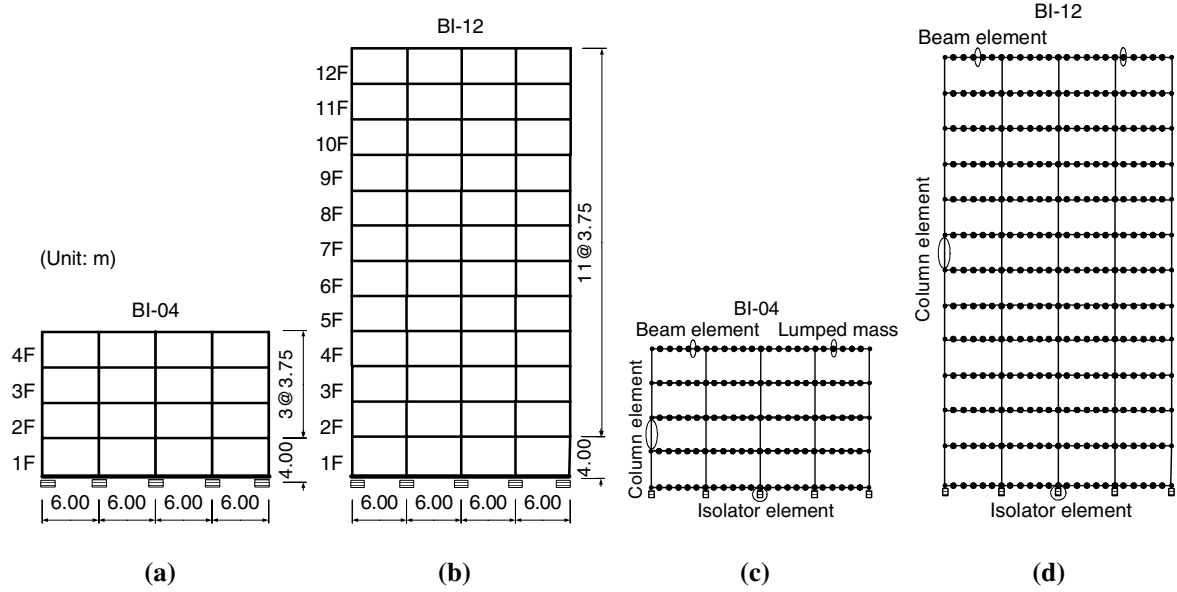


Fig. 7. Analyzed structures: (a) structure BI-04; (b) structure BI-12; (c) model BI-04; (d) model BI-12.

Table 1. Natural period of analyzed structure

	Base-fixed				Base-isolated			
	Horizontal		Vertical		Horizontal			Vertical
	1 st	2 nd	1 st	2 nd	10%	100%	250%	Compression
BI-04	1.23	0.46	0.24	0.22	1.56	2.63	2.99	0.24
BI-12	2.14	0.85	0.25	0.24	2.48	3.91	4.60	0.25

As shown in Fig. 7 (c) and (d), the superstructure was modeled by a series of column and beam elements with concentric plastic hinges assigned at each member end. Each beam was divided into six beam elements, and lumped mass was assigned at each joint to take into account the beam vertical vibrations. The basic parameters used to represent the hysteretic characteristics of the LRB are shown in Fig. 8(a), and the force-deformation relationship of the isolator element is shown in Fig. 8(b) and (c).

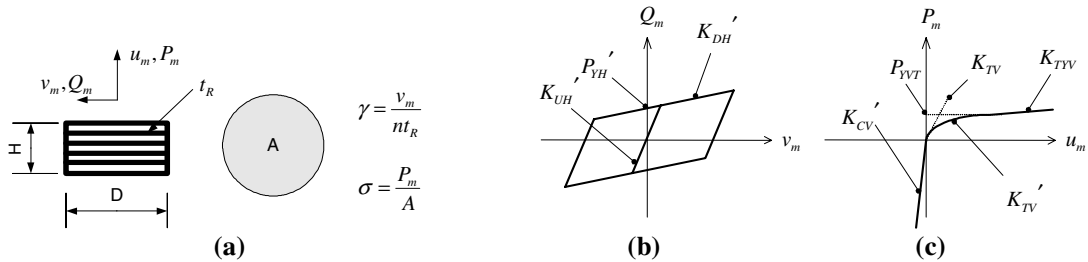


Fig. 8. Lead rubber bearing (LRB) model: (a) basic parameters; (b) horizontal force – deformation relationship; (c) vertical force – deformation relationship.

The modified bilinear model was used to represent the LRB's horizontal behavior [8]. K_{DH}' , P_{YH}' , and K_{UH}' shown in Fig. 8(b) are the post-yielding stiffness, yield force, and initial stiffness, respectively.

$$K_{DH}' = K_{DH} \times a_1(\gamma_{\max}) \times a_2(\sigma) \quad (1)$$

$$P_{YH}' = P_{YH} \times b_1(\gamma_{\max}) \times b_2(\sigma) \quad (2)$$

$$K_{UH}' = K_{UH} \times c \quad (3)$$

In Equations (1) to (3), $a_1(\gamma_{\max})$ and $b_1(\gamma_{\max})$ are the parameters to take into account the dependency of lateral stiffness on the lateral strain, $a_2(\sigma)$ and $b_2(\sigma)$ are the parameters to allow for the dependency of later stiffness on the vertical force, and c is a constant to relate the initial lateral stiffness with post-yielding lateral stiffness. As shown in Fig. 8(c), vertical force – displacement behavior in compression was taken to be linear with a parameter given as a function of the horizontal displacement [Equation (4)].

$$K_{CV}' = K_{CV} \times \left\{ 1 - \frac{2}{\pi} \left[\frac{v_m}{D} \sqrt{1 - \left(\frac{v_m}{D} \right)^2} + \sin^{-1} \left(\frac{v_m}{D} \right) \right] \right\} \quad (4)$$

A nonlinear function shown in Equation (5), which was proposed in [9], was used to model the vertical behavior in tension.

$$K_{TV}' = K_{TYV} + (K_{TV} - K_{TYV}) e^{\frac{K_{TYV} - K_{TV} - u_m}{B_{TYV}}} \quad (5)$$

Details of these parameters are shown in [10]. The isolator model above can take into account dependencies of the horizontal stiffness on the vertical force and horizontal displacement, and dependencies of the vertical stiffness on the horizontal displacement and vertical force.

Analysis results

A program code named “CLAP” [11] was used for the dynamic response analysis in this study. The base-isolator’s model presented above was incorporated into the program code. A set of ground motions recorded in the 1995 Hyogoken-Nanbu (Kobe) earthquake, including ten fault normal components and corresponding vertical components, were used in the analysis [4]. The structures were analyzed when subjected to both the horizontal (fault-normal) and vertical motions simultaneously.

Effects of vertical motions without tension in base-isolators

Vertical stiffness of the base-isolators degrades significantly when subjected to tension. In order to gain general understanding about the effects of vertical motions on the response of the base-isolated structures, the effects of tensile stiffness degradation was not taken into account in the first phase of analyses. The tensile stiffness of the base-isolators was assumed to be the same as the compressive stiffness and remain linear-elastic. The following two cases were analyzed, i.e., the case in which the structures were subjected to horizontal and vertical motion simultaneously (referred to as VH-6), and for comparison the case in which the structures were subjected to horizontal motion only (referred to as H-6). To characterize the difference between VH-6 and H-6, ratios of maximum story drifts obtained from VH-6 and H-6 were adopted as an index. Further, to make the results comprehensive, the responses were estimated statistically as “median” and “standard deviation (SD)” [12]. Here “median” refers to the exponent of the mean of the natural log values of all data, and “Standard deviation (SD)” refers to the standard deviation of the natural log values of all data and approximately equals the coefficient of variation. Statistical results show that all the median ratios are nearly equal to 1.0, and the SD’s of the ratios are less than 0.1. These observations indicate that the responses between VH-6 and H-6 are very similar, and the vertical ground motion has little effects on the maximum story drift of the base-isolated structures. Similar observations were obtained for conventional structures [3].

VH-6 and V-6 were also compared to evaluate the effects of vertical motion on beam vertical accelerations. Figure 9 shows the ratio of the maximum accelerations between VH-6 and V-6. Those of the base floor located immediately above the base-isolation layer, second, third, and roof floors are presented for BI-04. Similarly, the base, second, seventh, and roof floors are presented for BI-12. As shown in Fig. 9, the median ratios (VH-6 to V-6) are nearly 1.0 except for the base floor level. The SD’s of the ratios are smaller than 0.1, and approximately one quarter of the SD’s of the maximum beam vertical accelerations obtained from VH-6. The beam vertical accelerations at the base floor immediately

above the base-isolation layer are nearly the same as those at the top of the base-isolators because of the stiff beams arranged on top of the base isolation layer. In the analysis, the vertical stiffness of the base-isolators is constant all along for V-6, whereas it keeps changing according to the horizontal displacement of the base isolators for VH-6. It is for this reason that the beam vertical accelerations at base floor differ rather significantly between VH-6 and V-6. However, this does not affect the maximum beam vertical accelerations of the upper floors significantly, because these accelerations are controlled primarily by the superstructure's vertical vibration. In summary, the maximum beam vertical accelerations of the superstructure can be estimated from the analysis with vertical motions only. Note that, although vertical motions only are inadequate to estimate the vertical accelerations of the floor immediately above the base-isolation layer, the magnitude of accelerations is after all small in the first floor relative to in upper floors [10].

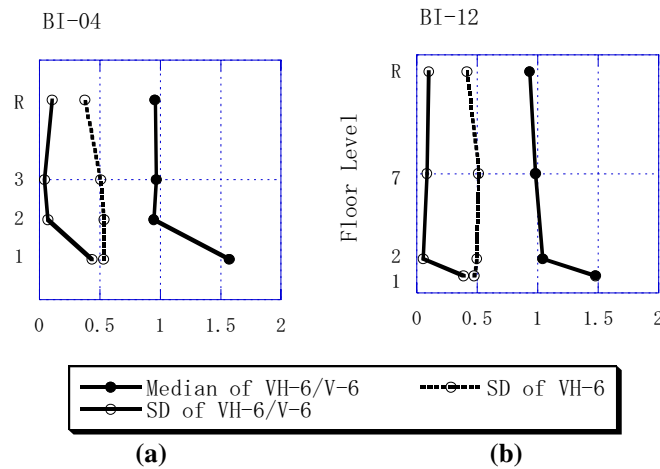


Fig. 9. Comparison of maximum beam vertical accelerations: (a) BI-4; (b) BI-12

Figure 10 shows the ratios of maximum beam vertical accelerations between the base-isolated and base-fixed structures. The median ratios are nearly 1.0 for all the floor levels of the superstructure. This observation indicates that the beam vertical accelerations of base-isolated structures are almost identical to those of the corresponding base-fixed structures. This observation is supported by the fact that the first vertical vibration period was almost identical between the base-isolated and base-fixed conditions (Table 1). This is because the first vibration mode was primarily the beam vertical vibration.

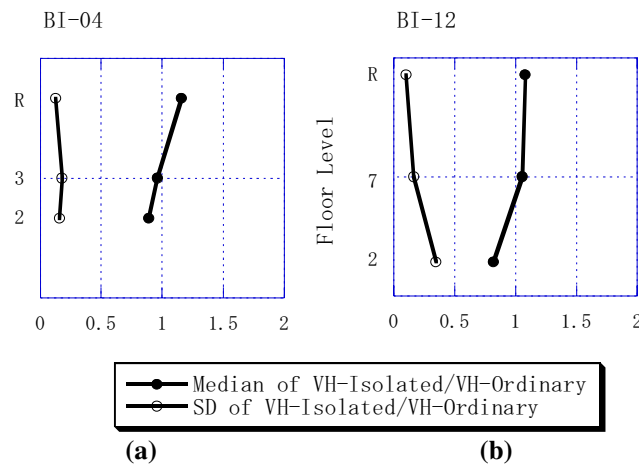


Fig. 10. Comparison of beam vertical accelerations between base-isolated and base-fixed structures: (a) BI-4; (b) BI-12.

Effect of vertical motions with tension of base-isolation layer

The model that took into account the vertical stiffness degradation due to tension was applied to the representative structures (BI-04 and BI-12), and the results are shown in Table 2. Each of the two base-isolated structures had three analysis cases, that is, horizontal motion only (H), vertical motion only (V), and horizontal and vertical simultaneously (VH). The results are given for each case and for each of the ten ground motions. The table shows the maximum tensile displacement of the base-isolators when tension occurred in the base-isolation layer. The cases when no tension occurred are marked by “X”.

Table 2 shows that no tension occurred for all three cases of BI-04 (the four story model) and V (vertical motion only) of BI-12 (the twelve story model). Seven out of ten ground motions involved tension for H (horizontal motion only) of BI-12, and nine out ten ground motions involved tension for VH of BI-12. It is also notable that the tensile displacements of VH are significantly greater than those obtained for H in most cases involving tension. This observation suggests that horizontal motions are the primary source that produces significant tension in the base-isolators, and vertical motions make the situation more promoted.

Table 2. Occurrence of tensile displacements (mm)

Record	BI-04			BI-12		
	H	V	VH	H	V	VH
Fn-amc	X	X	X	X	X	0.03
Fn-ekb	X	X	X	3.91	X	7.26
Fn-kb3	X	X	X	7.02	X	5.92
Fn-kbu	X	X	X	X	X	X
Fn-kob	X	X	X	X	X	0.18
Fn-koj	X	X	X	5.06	X	10.79
Fn-pr1	X	X	X	0.26	X	0.40
Fn-rki	X	X	X	3.97	X	4.25
Fn-tkt	X	X	X	1.49	X	4.92
Fn-tzk	X	X	X	0.56	X	2.09

Effect of tension on story drift and beam accelerations

The vertical stiffness degrades to about 2% of the compressive stiffness when sustaining tension, and the yield tensile force is small. In order to investigate the potential effect of tension on the maximum story drift and beam acceleration of the superstructure, two cases, one including tensile stiffness degradation (designated as “tension”) and the other not including the degradation (designated as “no-tension”), were compared. Here focused was VH of BI-12 for the nine ground motions involving tension (Table 2). The ratios of responses obtained from “tension” and “no-tension” were adopted as indices for comparison.

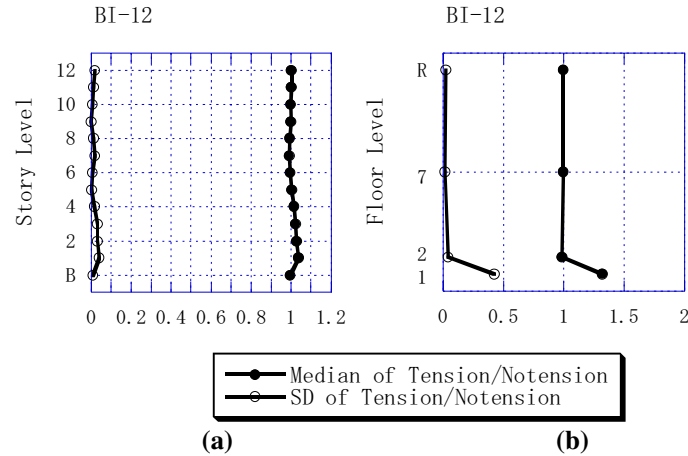


Fig. 11. Comparison between “tension” and “no-tension”:
(a) maximum story drift; (b) beam vertical acceleration

Fig. 11 shows the medians and SD's of the ratios. Figure 11(a) is for the maximum story drift and Fig. 11(b) is for the maximum beam vertical acceleration. In Fig. 11(a), all the median ratios are nearly 1.0 and the SD's are smaller 5%. In Fig. 11(b), all the median ratios of the superstructure are almost identical to 1.0, and the SD's are nearly zero, but the median ratio at the base floor is about 1.4, and the corresponding SD's is 0.4. These observations indicate that the effects of tension on the maximum story drift are minimal for both the superstructure and base-isolation layer. Tension involves significant increases of beam vertical accelerations at the base floor but does affect little the beam vertical accelerations of the superstructure. The relatively large accelerations in the base floor were a result of bumping at that floor level, which occurred when the base-isolator's stress changed from tension to compression. The tensile stiffness was much smaller than the compressive stiffness; thus a sudden change in vertical stiffness (from tension to compression) caused large accelerations. However, that the magnitude of accelerations is after all small in lower floors relative to in upper floors [10]. Thus, the increase of acceleration observed in lower stories is not critical in the estimation of beam maximum vertical acceleration. In summary, tension has no significant effect on beam vertical accelerations.

CONCLUSIONS

This paper presented two issues of concern related to the application of base-isolated building structures, and the following conclusions are obtained.

1. Many fault-normal components of near-fault ground motions recorded in previous earthquakes provided the base-isolation layer of base-isolated building structures with maximum horizontal displacements of not smaller than 0.5 m, a commonly adopted clearance between the structure and surrounding retaining walls.
2. The response behavior of the base-isolated structure when collided with the surround walls was greatly affected by the resisting characteristics of the walls including the soils behind the walls. Detailed FEM analyses indicated that the wall's stiffness and strength (including those of the soils) were about 30 to 60% and 60 to 300% of the stiffness and strength of the superstructure whose first natural period is 0.5 sec and yield base shear coefficient is 0.3.
3. In most cases, the number of collisions was limited to one to two, because the primary ground motions were short in primary motions. Relationships between the level of input ground motions and the expected horizontal deformations of the base-isolation layer and superstructure were presented.

4. A detailed model that represents the hysteretic behavior of base-isolators when subjected to axial and horizontal loads simultaneously was developed and used for dynamic response analyses of base-isolated structures when subjected to both the horizontal and vertical ground motions. Story drifts of the superstructure were not affected by vertical ground motions.
5. Beam vertical accelerations remained unchanged between the base-isolated and base-fixed structures. Tensile forces occurred in base-isolators for tall buildings because of overturning moment, while no tension occurred with vertical ground motions only. Tensile forces provide amplification of maximum vertical accelerations in the floor immediately above the base-isolation layer; otherwise practically no effect was observed as to the maximum story drifts or the maximum beam vertical vibration of the superstructure.

REFERENCES

1. Pan P, Zamfirescu D, Nakashima M, Nakayasu N. "Base-Isolation design practice in Japan: introduction to the post-Kobe approach." *Journal of Earthquake Engineering* (accepted for publication).
2. Hall JF, Heaton TH, Halling MW, Wald DJ. "Near-source ground motion and its effects on flexible buildings." *Earthquake Spectra* 1995, 11(4): 569-605.
3. Pan P, Nakashima M. "Effect of vertical vibration on story drift, column axial force and beam acceleration of steel moment frames subjected to near-fault motions." *The Fourth International STESSA, Naples, Italy, Jun. 2003: 541-546.*
4. Nakashima M, Matsumiya T, Asano K. "Comparison in earthquake responses of steel moment frames subjected to near-fault strong motions recorded in Japan, Taiwan, and the U.S.." *International Workshop on Annual Commemoration of Chi-Chi Earthquake, Taipei, Taiwan, September 18-20, 2000: 112-123.*
5. Nakayasu N, Nakashima M. "Response characteristics of base-isolated building structure including collisions with retaining wall." *Summary of National Convention of Architectural Institute of Japan, September 2003: 441-442 (in Japanese).*
6. MSC.MARC online manual. Japan MSC Co., 2001.
7. Nakayasu N, Pan P, Nakashima M. "Response and damage of base-isolated buildings subjected to very large earthquakes." *Proceedings of Tenth Anniversary Conference of the Japan Society for Seismic Isolation (in press).*
8. "Design Methods for Response Controlled Structures". Japan Structural Consultants Association, Shokokusha, 2000 (in Japanese).
9. Kikuchi M, Kitamura Y. "Mechanical characteristics of electrometric seismic isolation bearings under tension." *Journal of Structure and Construction Engineering, AIJ, 1999, 10(24): 57-64 (in Japanese).*
10. Pan P, Nakashima M, Tada M. "Effects of vertical ground motions on response of base-isolated structure". *Journal of Structural Engineering* 2004, 50B: 404 (in press).
11. Ogawa K, Tada M. "Computer program for static and dynamic analysis of steel frames considering the deformation of joint panel." *Proceedings of the Seventeenth Symposium on Computer Technology of Information, Systems and Applications, AIJ, Dec. 1994 (in Japanese).*
12. Luco N, Cornell CA. "Effect of connection fractures on SMRF seismic drift demands". *Journal of Structural Engineering ASCE* 2000; 126(1): 127-136.